

Hot pressing of isothermally solidified Ge-Si alloys

F. A. A. AMIN, M. A. A. ISSA, A. M. HASSIB, Z. H. DUGHAISH
*Materials Study Group, Department of Physics, Faculty of Science,
King Saud University, PO Box 2455, Riyadh, Saudi Arabia*

Germanium-silicon alloys of nominal composition $\text{Ge}_{50}\text{-Si}_{50}$ atomic fraction have been prepared by isothermal solidification and hot-pressing at temperatures up to 1350 K and pressure of 178 MPa. It is shown that high degree of homogenization can be obtained in the final compact. This work lends further evidence for the plastic flow mechanism of the sintering of these alloys.

1. Introduction

Heavily doped germanium-silicon alloys may be considered to be the only available thermoelectric alloys for use at high temperature in excess of 1300 K. An established procedure for hot-pressing of alloys suitable for device application uses alloys produced by either zone levelling [1-3] or chill casting [4-6]. The choice of zone levelling or chill casting is a direct consequence of the wide separation of the solidus/liquidus lines in the phase diagram. The alloys are then milled to a powder of particle size less than $40\ \mu\text{m}$ followed by hot-pressing at temperatures near or in excess of the solidus temperature and pressures of up to 340 MPa. Densities approaching theoretical values have been reported using the above procedure. The significance of hot-pressing is that a controlled concentration of grain boundaries can be introduced which results in an increase in grain boundary phonon scattering.

The main difficulties associated with the growth of homogeneous alloys are the low distribution coefficient of germanium in silicon (0.33) [7], the low diffusion coefficient of the component elements in the solid ($10^{-6}\ \text{m}^2\ \text{sec}^{-1}$) [8] and the wide separation of the solidus/liquidus. The structure often encountered in these alloys is the dendritic type formed as a result of constitutional supercooling [9]. The solidification process is further complicated by the difference in densities of the component ele-

ments which result in gravity segregation of the heavier element germanium. Zone levelling as applied to complete solid solutions [10, 11] can produce alloys with the required homogeneity but the cost and time involved in this process prohibits its exploitation as a viable method and limits its use to laboratory studies. Chill casting, on the other hand, presents a more attractive alternative although segregation is never completely suppressed and impurity pick up from the mould can be a serious problem if copper moulds are used.

As an alternative to zone levelling and chill casting, it was decided to investigate the structure and homogeneity of isothermally solidified and hot-pressed alloys of $\text{Ge}_{50}\text{-Si}_{50}$ atomic fraction.

Despite the importance of Ge-Si alloys, important information regarding the sintering mechanism appears to be lacking and most reported hot-pressing temperatures fall just below or above the solidus temperature. From the fundamental point of view, it is not appropriate to compare hot-pressing in the solid state with that where liquid phase is present since different parameters are operative in the two modes. The present work carried out entirely below the solidus temperature lends evidence to the model of plastic flow originally proposed for Ge-Si alloys by Sahm and Gnau [5] and subsequently expounded by Savvides and Goldsmid [6]. The approach adopted in this work is to treat

the entire process from growth of the alloy to the hot-pressed end product as an integrated process and to aim for homogeneity in the final end product, the hot-pressed alloy.

2. Experimental procedure

2.1. Alloy growth

The appropriate weight fractions of elemental silicon and germanium (total weight 62×10^{-3} kg) to give an alloy of 50/50 atomic fraction together with the required amount of boron dopant are placed inside a high purity fused clear silica crucible. Prior to every melt the crucible is given a thorough cleaning in a 10% HF solution followed by a rinse in distilled water and ethanol. The starting materials are all spec-pure with total impurities not exceeding 2 ppm. The starting material and crucible are placed inside a high purity graphite susceptor previously degassed at temperatures in excess of the highest temperature required to melt the charge. The graphite susceptor is surrounded by graphite-woven felt and an alumina tube to stop radiative heat transfer to the r.f. coil which surrounds the alumina tube. The entire assembly is located inside a vacuum chamber which can be evacuated to better than 10^{-5} torr using a rotary/diffusion train. The power source is a 30 kW, 365 kHz, r.f. generator connected to the work coil via ceramic feed-through insulators, through the water-cooled wall of the vacuum chamber. The vacuum chamber incorporates viewing ports so that a check on the progress of solidification can be made.

A typical melting and solidification run consists of first evacuating the chamber to better than 10^{-5} torr followed by an argon flush, re-evacuation and finally filling to atmospheric pressure with purified argon gas (impurity ≤ 1 ppm). The purity of the argon and the partial pressure of the residual gases in the chamber are monitored using a quadrupole micromass head located just below the liquid nitrogen trap that separates the chamber from the diffusion pump. Heating to 150 K above the liquidus temperature is accomplished within 45 min followed by a 30 min hold at this temperature where r.f. stirring ensures a thorough mixing of the melt. The desired rate of solidification is accomplished using either an open loop (motorized r.f. power control) or a closed loop (digital heating/cooling programmer) system via a Pt/Pt-13% Rh ther-

mocouple located inside the susceptor at a distance of 5 mm below the crucible, to control the temperature. The controlled rate of solidification is applied to the region starting at 50 K above the liquidus and ending 100 K below the solidus. The remaining temperature range is cooled at a rate of 20 K min^{-1} .

2.2. Alloy reduction

The ingot is first broken down into small pieces not exceeding 2×10^{-3} m across using an agate hand mortar and pestle. The crushed ingot, together with a mix of agate balls ranging in size from 5 to 20×10^{-3} m, are loaded into agate vessels and the entire contents sealed using teflon seals. Milling is achieved using a planetary mill for a period of 60 min.

2.3. Powder grading

Wet sieving using microsieves and ethanol was used to separate the different fractions. The sieves used are pure nickel screens electrolytically formed and supported on stainless steel circular frames. The sieves employed range in size from 5 to $100 \mu\text{m}$. Sieving was accelerated by the use of an electromagnetic vibrator oscillating at a fixed frequency of 6 kHz. The use of ethanol minimizes blockage of the apertures and reduces abrasion of the screens thus reducing powder contamination. Ethanol is separated from the sieved fraction by distillation, and final drying is achieved by open evaporation using magnetic stirring and heating to reduce sedimental agglomeration.

2.4. Hot-pressing

The hot press is shown in Fig. 1. The die assembly is made entirely of Ti-Zr-Mo (TZM) alloy and consists of bottom plunger (1), die cylinder (2) and top plunger (3). The die cylinder has a nominal diameter of 25×10^{-3} m and is lined with a tube of high purity poco graphite (4). The faces of the upper and lower plungers are also lined with thin discs of poco graphite (5). Any wear in the graphite components is compensated for by the use of thin 25×10^{-3} m thick flexible graphite foil. Heat flow from the upper and lower plungers is reduced by the use of ceramic and mica discs positioned at heat sensitive locations. A graphite susceptor and graphite felt surrounds the die assembly (6), and the entire assembly is located inside a double

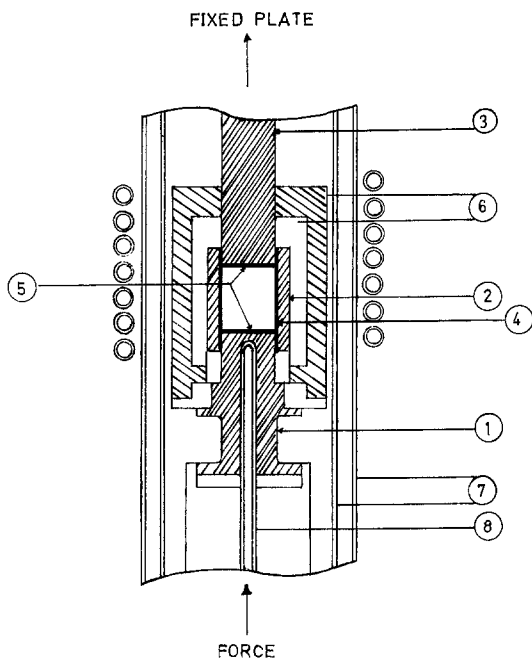


Figure 1 Schematic arrangement of hot press and die assembly.

walled water-cooled silica cylindrical vacuum enclosure (7). The seven-turn r.f. coil is positioned outside the vacuum enclosure. The entire assembly is mounted on the lower plate of the four column hand-operated hydraulic press of 20×10^4 N force. The load is transmitted to the die assembly via a sliding vacuum seal. The vacuum system to the hot press is the same system employed for the alloy growth chamber and thus the same conditions prevail. The temperature of the die assembly is monitored by a Pt-6% Rh/Pt-30% Rh thermocouple located inside the lower plunger (8). All graphite components are degassed at temperatures 100 K above the hot-pressing temperatures to minimize contamination of the charge. The design of the die assembly permits loading and plunger alignment outside the hot press.

A typical pressing procedure consists of first evacuation of the chamber to better than 10^{-5} torr followed by argon flushing and re-evacuation. A load of 5×10^3 N force is applied without heating followed by heating to 973 K. At this temperature a force of 4×10^4 N force is applied and heating continued until the final hot-pressing temperature is reached at which time the full load (9.2×10^4 kgf) is applied. The load is maintained constant to better than

250 kgf and the temperature regulated so as not to exceed ± 2 K for a period of 60 min. The heating to the desired temperature takes 60 min. At the end of the pressing period the load is first removed followed by switching off the r.f. power. Cooling to room temperature takes another 60 min.

3. Analytical procedure

3.1. Metallography

Specimens for metallographic examination are cut using either a slow speed diamond disc saw or diamond-coated wire saw. Small specimens are usually mounted in acrylic resin to facilitate handling. Grinding and polishing is carried out using diamond spray or paste until a finish of $0.25 \mu\text{m}$ is produced. To reveal the structure one of two etchants is used, the first is CP4a, and the second is locally developed and is made up of 10^{-2} kg FeCl_3 , 25×10^{-6} m³ distilled water, 10^{-5} m³ HF and 10^{-5} m³ HCl. The latter etchant will be referred to as FeIII.

3.2. X-ray diffraction

Samples for X-ray analysis are first crushed using an agate ball mill for a period of 1 h. The resulting powder is mixed with 2 parts by volume of acrylic powder and the mixture is hot-pressed using a metallurgical mounting press at temperatures of 453 K and a pressure of 60 MPa. This produces discs 2 to 3×10^{-3} m thick and suitable for direct mounting on the vertical Phillips powder diffractometer. Filtered $\text{CuK}\alpha$ radiation is used and the angular range 2θ from 20° to 100° is usually scanned. The diffraction pattern is recorded on a chart paper moving at either 2×10^{-2} m/ $1^\circ 2\theta$ or 8×10^{-2} m/ $2^\circ 2\theta$. A Nelson-Riely extrapolation function is used to obtain corrected value of lattice parameter. The accuracy of the diffractometer is frequently checked using a standard silicon sample.

3.3. Density measurement

The density of an irregularly shaped specimen is obtained by method of hydrostatic weighing. For specimens that have well characterized dimensions, density is obtained by weighing and measurement of external dimensions.

4. Results and discussion

The main factor causing inhomogeneity in Ge-Si alloys is constitutional supercooling and,

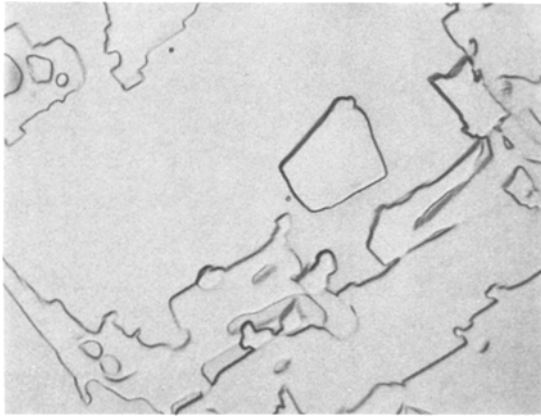


Figure 2 Photomicrograph of isothermally solidified Ge₅₀-Si₅₀ alloy. Etched in CP4a. $\times 450$.

as shown by Dismukes and Ekstrom [3], alloys with composition near the 50/50 atomic fraction are more difficult to homogenize. In material homogenized by zone levelling the growth rate required for such alloys was 100 times slower than for dilute alloys. The alloys employed for this work are nominally 50/50 atomic fraction. Several cooling rates were employed ranging from 10 to 0.25 K min⁻¹. It was found that suppression of dendrite formation was obtained at a cooling rate of (1 K min⁻¹). Metallographic examination of a longitudinal section through the ingot shows the complete absence of dendrites and Fig. 2 shows a typical microstructure. This microstructure shows large angular grains which appear to be very similar to the structure of a zone-levelled material. The origin of these large grains is believed to be dendrites broken up during the isothermal solidification. The critical factor in breaking up these dendrites is the r.f. stirring. This point was confirmed by remelting an r.f. homogenized ingot in a resistance heated furnace. All the melting and solidification parameters were kept identical. The resulting structure showed several dendrites extending along the entire length of the ingot.

As germanium is the first element to melt, a thin layer of germanium coats the sides of the crucible which has the beneficial effect of inhibiting contamination of the charge from the crucible. However a somewhat thicker layer of germanium appears to settle at the bottom of the crucible due to gravity segregation, and X-ray examination of this layer revealed the existence of a germanium-rich phase in addition to the main

phase. Inverting the ingot and remelting did not suppress the formation of this germanium-rich phase and the only way to eliminate it was to cut off 2×10^{-3} m from the bottom of the ingot. The main criterion used in this work in assessing the suitability of the ingot for hot-pressing is to examine the powder by X-ray diffraction after the ingot has been reduced to its final particle size. If the pattern shows a single phase, even though the peaks may be broader, then the powder is used for hot pressing. Peak broadening is due to the existence of microscale segregation within a single grain rather than the existence of a distinct second phase. Comparison of X-ray diffraction patterns and lattice parameter calculation between powders of different particle size originating from the same ingot did not reveal any measurable variation in composition. This is probably an indication that the microscale segregation does not exceed the smallest size of grains of $\sim 5 \mu\text{m}$.

In evaluating the hot-pressing parameters, three different compacts were used. B 11 and B 13 originate from the same ingot but differ in particle size, pressing temperature and pressure. B 41 originates from a different ingot but of similar nominal composition. The chemical compositions of these three compacts were obtained by fitting their lattice parameter values into the data of Dismukes *et al.* [12]. As can be seen from Table I, B 11 and B 13, although having different particle sizes, have a chemical composition difference of 0.3 at % germanium. Compact B 41 appears to have a composition well within the range of the previous two indicating that the process used from alloy growth to final compact does not involve any losses. The close agreement in chemical composition between B 11 and B 13 indicates that the ingot had started as a single phase. Otherwise had the ingot started as a two-phase alloy, preferential milling would have taken place as reported by Lefever *et al.* [4].

Fig. 3 shows the end point relative density, D_{∞} , which is the ratio of measured density to the bulk density. This indicates that the density is temperature dependent and in agreement with previously reported data [6]. Variation of density within one compact along the pressing direction was measured on slices 2×10^{-3} m thick. The curve of density against position is shown in Fig. 4. With the exception of one point, all the

TABLE I

Sample	Composition (at % Ge)	Particle size (μm)	Pressing temperature (K)	Pressure (MPa)	Measured density ($10^{-9} \text{ kg m}^{-3}$)	Bulk density ($10^{-9} \text{ kg m}^{-3}$)	Lattice parameters (nm)	End point density (D_{∞})	FWHM (220) (deg 2θ)	Yield stress, τ_c (MPa)
B 11	53.7	-5	1291	173	3.3655	4.01175	0.55486	0.84	0.4	66.0
B 13	54.0	-15+10	1301	178	3.5017	4.02622	0.554926	0.87	0.5	61.6
B 41	53.5	-5	1349	177	3.9111	4.01154	0.554815	0.97	0.5	46.5

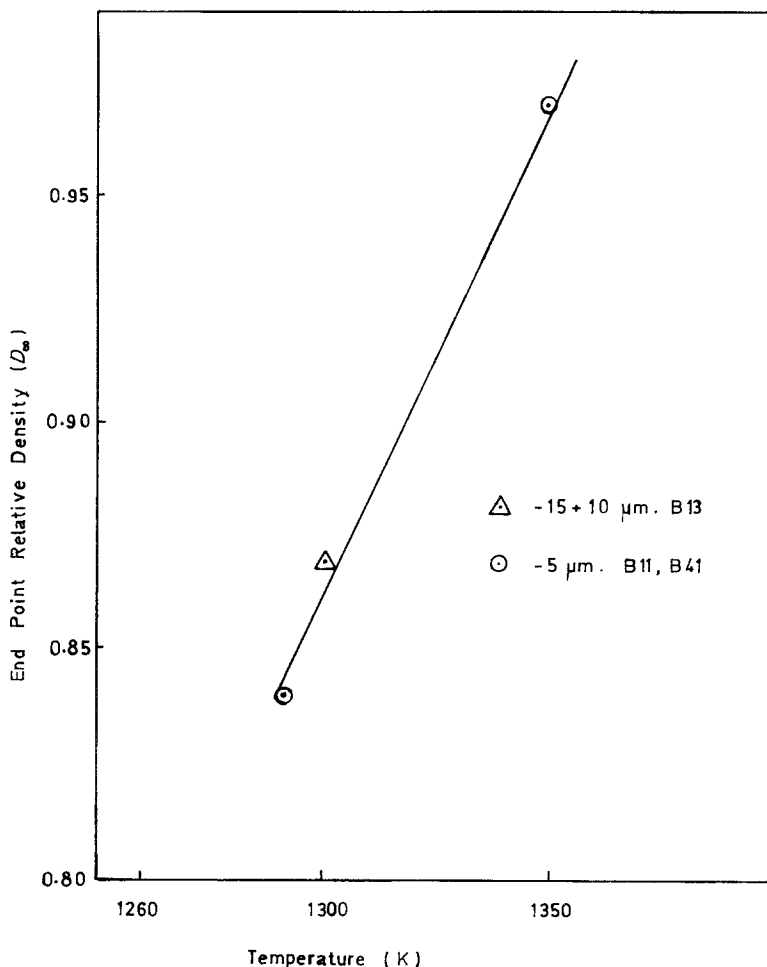


Figure 3 Plot of end-point relative density against pressing temperature.

density values fall on a straight line. The maximum deviation from average density is 1.5%. In deriving the bulk density corresponding to the particular composition, the chemical compositions as obtained from lattice parameter values are fitted into the density versus composition data of Dismukes *et al.* [12].

Metallographic examination of an etched section perpendicular to the pressing direction (Fig. 5) shows a grain structure resembling that of the unpressed powder with no signs of grain growth. Some entrapped porosity is apparent which is indicative of the fact that sintering is a non-diffusion based process, otherwise pore intercorrection should be apparent. Microscopic examination of unetched B 41 shows a complete absence of porosity as this compact has a value of D_{∞} of 0.97. The results from the present work cover a composition range not previously studied in detail. As pointed out previously, the dis-

tribution of porosity suggests that a sintering model based on diffusion and migration of vacancies is not appropriate. Savvides and Goldsmid [6] considered a sintering model based on plastic flow as originally proposed by Mackenzie and Shuttleworth [13] and extended to hot-pressing by McClelland [14]. This model, as refined by Savvides and Goldsmid [6], appears to fit their data as well as that of Sahm and Gnau [5], equally well although their two sintering parameters are different. Fig. 6 shows a graphical representation of the equation proposed by Savvides and Goldsmid [6]

$$\left[\ln \left(\frac{1}{\phi_{\infty}} \right) - \ln (1 - \phi_0) \right] (1 - \phi_{\infty}^{2/3}) = p / \sqrt{2} \tau_c \quad (1)$$

where ϕ_0 is the porosity at zero pressure and equals $1 - D_{\infty}(0)$ and $D_{\infty}(0)$ is the relative density at zero pressure.

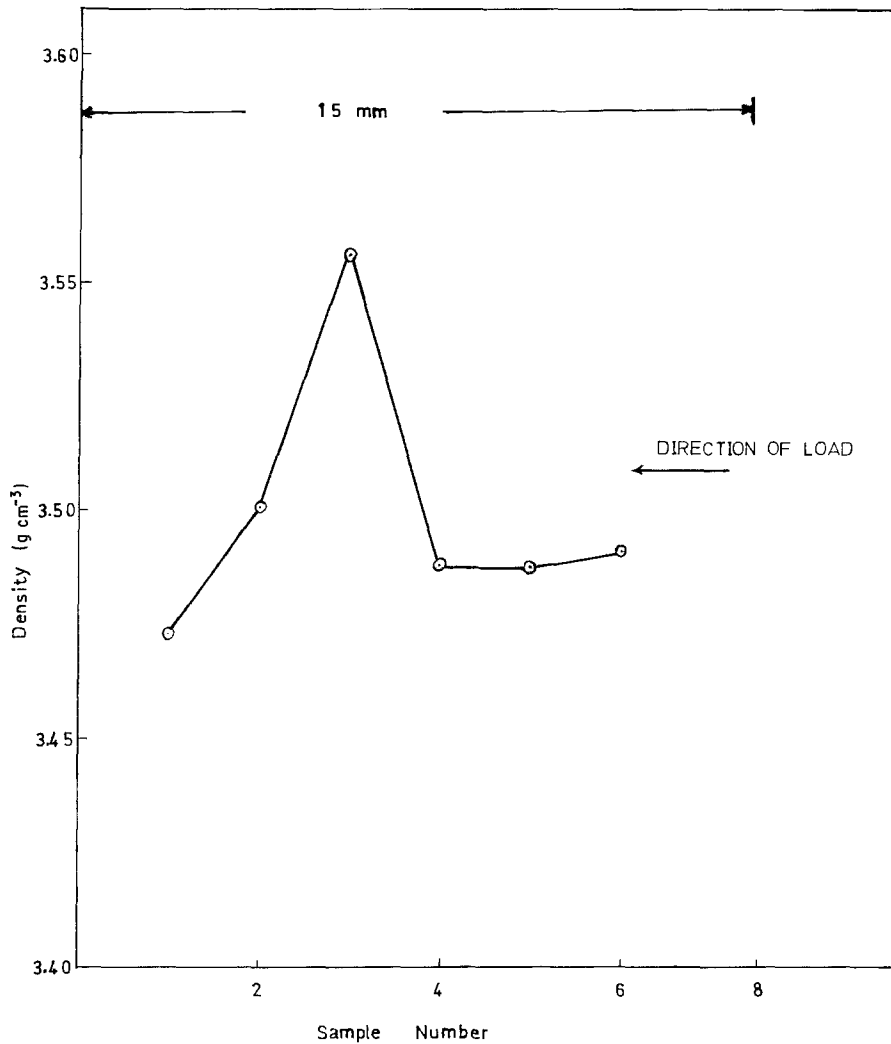


Figure 4 Plot of density against position along the pressing direction within the compact.

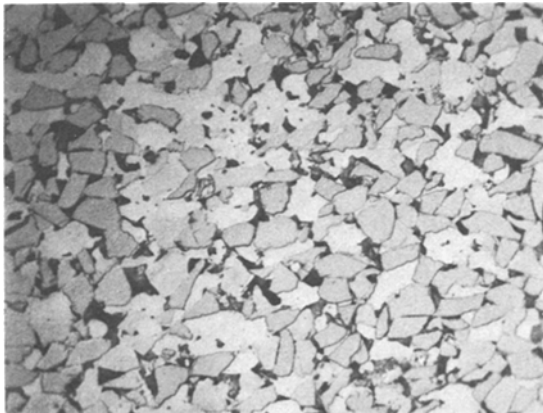


Figure 5 Grain structure of hot-pressed B13 sample. Etched in FeIII. $\times 550$.

The value of ϕ_0 was given to be 0.51 and the same value used in our calculation. D_∞ is the end point relative density and $\phi_\infty = (1 - D_\infty)$, τ_c is the yield stress and P the pressure. In calculating the values of yield stress τ_c corresponding to the temperature used in this work, i.e. 1291, 1301 and 1349 K, the data of Savvides and Goldsmid [6] were plotted as an Arrhenius relationship and the values of τ_c corresponding to our temperatures were obtained by regression analyses and linear interpolation on a $\ln \tau_c$ against $1/T \text{ K}^{-1}$ graph. The values corresponding to different temperatures are given in Table I. It appears that our data fit very well the line corresponding to 1349 K and a reasonably good fit is obtained for the other two temperatures, i.e.

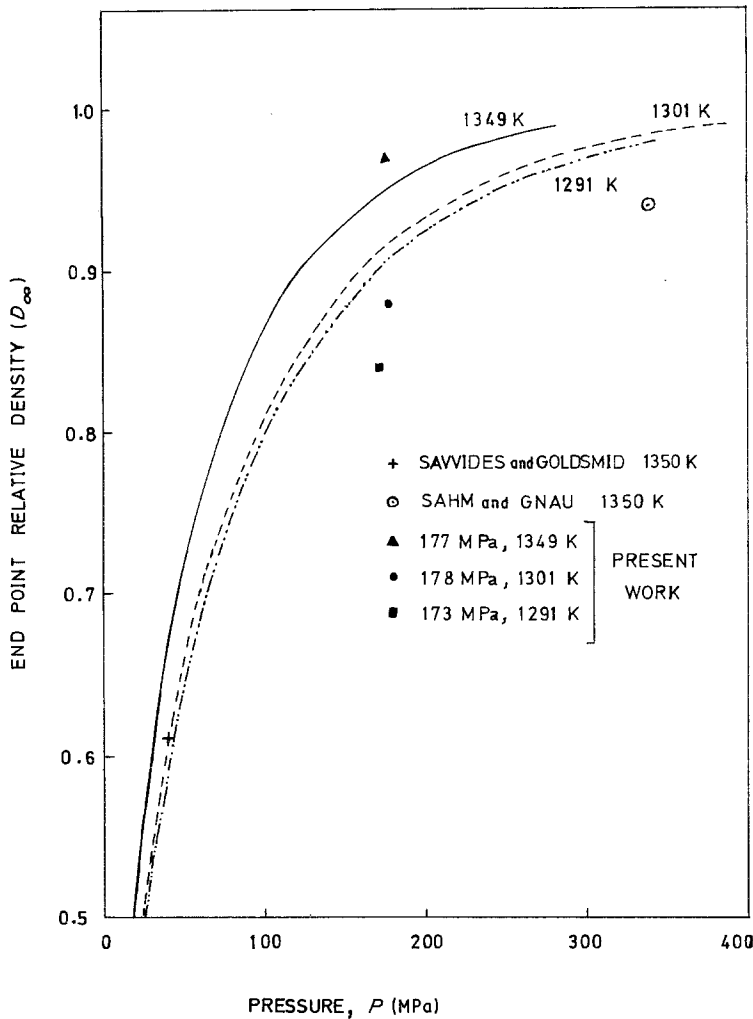


Figure 6 Plot of end point relative density, D_{∞} , against pressure according to Equation 1.

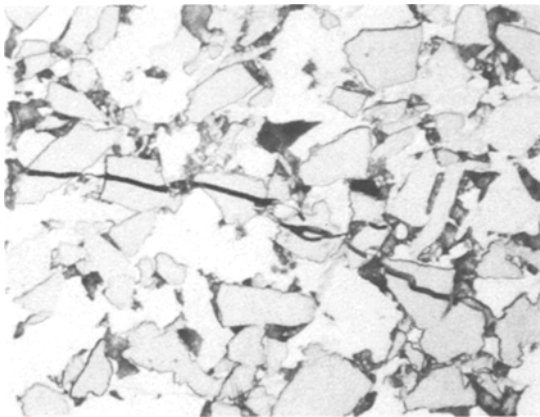


Figure 7 Cracked grains in B13 compacts. Etched in FeIII. $\times 1125$.

1291 and 1301 K. Without a doubt, this model appears to fit data covering widely varying compositions and pressing parameters and the deviation of some points from the graph may be associated with values of the parameter τ_c . Further evidence in support of this model is given in Fig. 7 which shows compact B 13 at a magnification of $\times 1125$. Some grains show clear signs of grain fragmentation caused by high pressure, 178 MPa, and a low pressing temperature of 1301 K. The low temperature results in a low degree of plasticity causing the grains to crack instead of plastically flowing. During pressing, a certain degree of homogenization appears to take place as shown by the sharpness of the X-ray peaks in Fig. 8, which shows peaks having

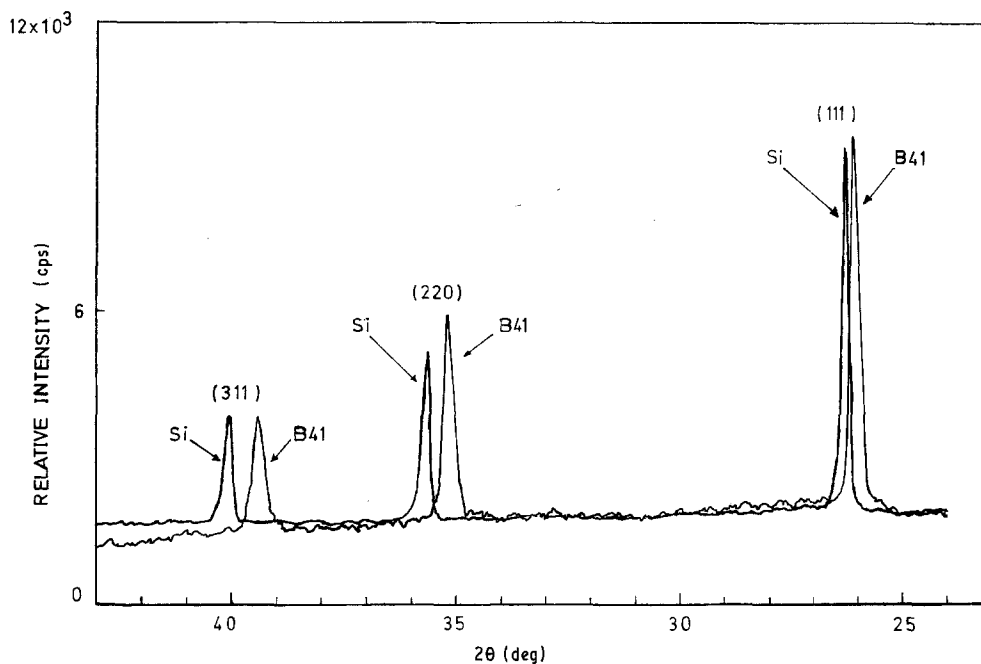


Figure 8 X-ray profiles of pure silicon and B 41 compact after hot-pressing.

full width at half maximum (FWHM) comparable to that of pure silicon. This homogenization is taking place within each individual grain and this is distinct from sintering by diffusion which takes place between neighbouring grains. This point confirms our deduction that the segregation in the solidified ingots is on a microscale and within each individual grain.

5. Conclusions

This work shows that completely homogeneous Ge-Si alloys can be prepared by isothermal solidification followed by hot-pressing. Any segregation that cannot be removed by isothermal solidification is eliminated during hot-pressing. The Mackenzie-Shuttleworth-McClelland model [13, 14] is further established, and further work to determine the electrical and thermal behaviour of these alloys will be published.

Acknowledgements

The authors would like to thank the Vice-Rector of the King Saud University, Dr S. Al-Athel, for support and encouragement, Dr D. M. Rowe of UWIST for valuable advice, and the Saudi Arabian Centre for Science and Technology for financial support (grant AT/4-42).

References

1. D. M. ROWE and R. W. BUNCE, *J. Phys. D. Appl. Phys.* **2** (1969) 1497.
2. R. W. BUNCE and D. M. ROWE, *J. Appl. Phys.* **10** (1977) 941.
3. J. P. DISMUKES and L. EKSTROM, *Trans. Met. Soc. AIME* **233** (1965) 672.
4. R. A. LEFEVER, G. L. MCVAY and R. J. BAUGHMAN, *Mater. Res. Bull.* **9** (1974) 863.
5. P. R. SAHM and L. H. GNAU, *Z. Metallkde.* **59** (1968) 137.
6. N. SAVVIDES and H. J. GOLDSMID, *J. Mater. Sci.* **15** (1980) 600.
7. F. A. TRUMBORE, *Bell System Tech. J.* **39** (1960) 205.
8. H. STOHR and W. KLEMM, *Z. Anorg. Chem.* **241** (1939) 313.
9. B. CHALMERS, "Principles of Solidification" (Wiley, New York, 1964).
10. C. C. WANG and B. H. ALEXANDER, Bureau of Ships, Contract No. 63180 (1955) US Navy, Washington.
11. G. BUSH and O. VOGT, *Helv. Phys. Acta* **33** (1960) 537.
12. J. P. DISMUKES, L. EKSTROM and R. J. PAFF, *J. Phys. Chem.* **68** (1964) 3021.
13. J. K. MACKENZIE and R. SHUTTLEWORTH, *Proc. Phys. Soc. B.* **62** (1949) 833.
14. J. C. McCLELLAND, "Powder Metallurgy", edited by W. Leszynski (Interscience, New York, 1961) p. 157.

Received 16 October 1984
and accepted 10 January 1985